

Supporting Information

Enhancing Co/Co₂VO₄ Li-ion Battery Anode Performances *via* 2D-2D

Heterostructure Engineering

Kun Wang[#], Yongyuan Hu[#], Jian Pei^{*}, Fengyang Jing, Zhongzheng Qin, Huabin Kong, Jinli Wang,
Yumin Zhou, and Gang Chen^{*}

MIIT Key Laboratory of Critical Materials Technology for New Energy Conversion and Storage,
School of Chemistry and Chemical Engineering, Harbin Institute of Technology, Harbin 150001, P.
R. China

E-mail: peijian@163.com and gchen@hit.edu.cn

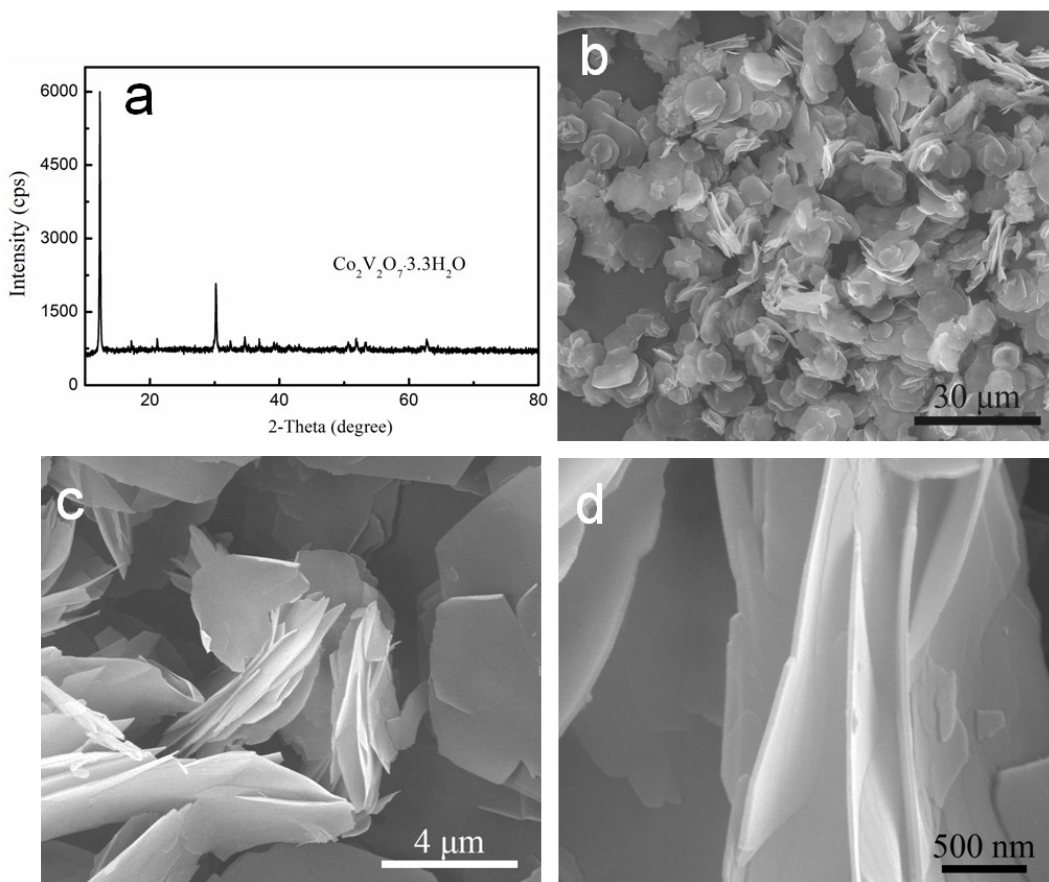


Figure S1. Phase and morphological characterizations of the as-prepared $\text{Co}_2\text{V}_2\text{O}_7 \cdot 3.3\text{H}_2\text{O}$ precursor: (a) XRD pattern, (b-d) SEM images.

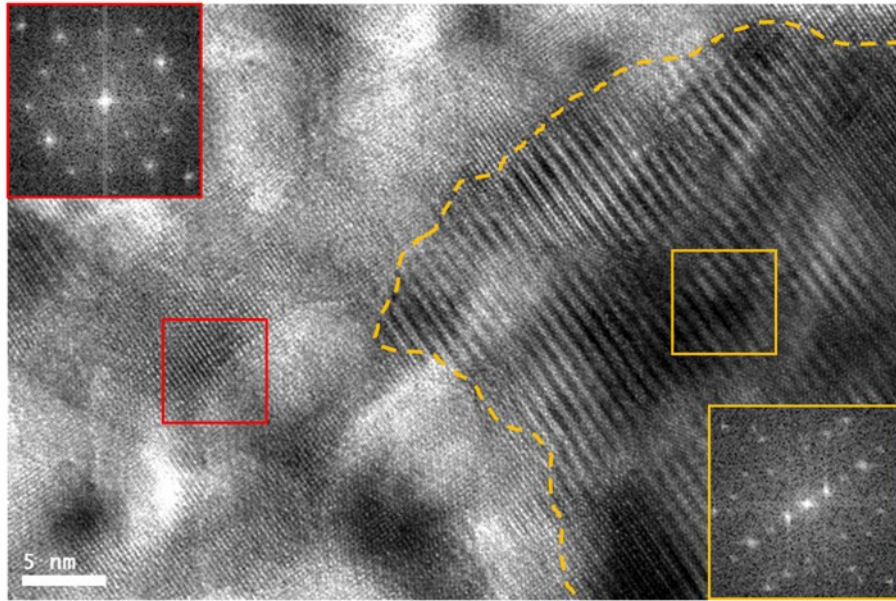


Figure S2. HRTEM image of CVO-400, inset: FFT images taken from different regions.

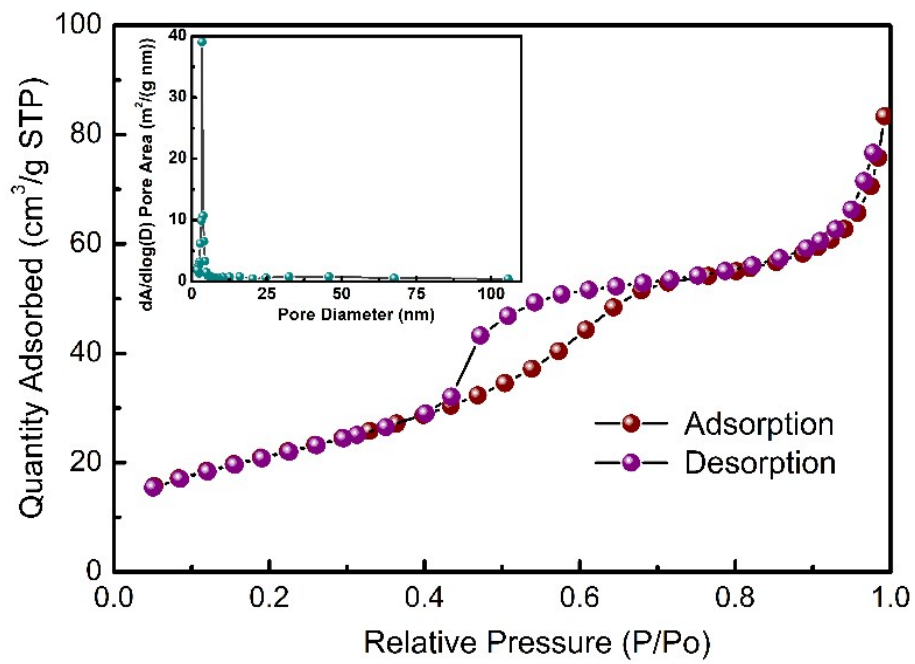


Figure S3. Nitrogen adsorption/desorption isotherm and pore size distributions (inset) of CVO-350.

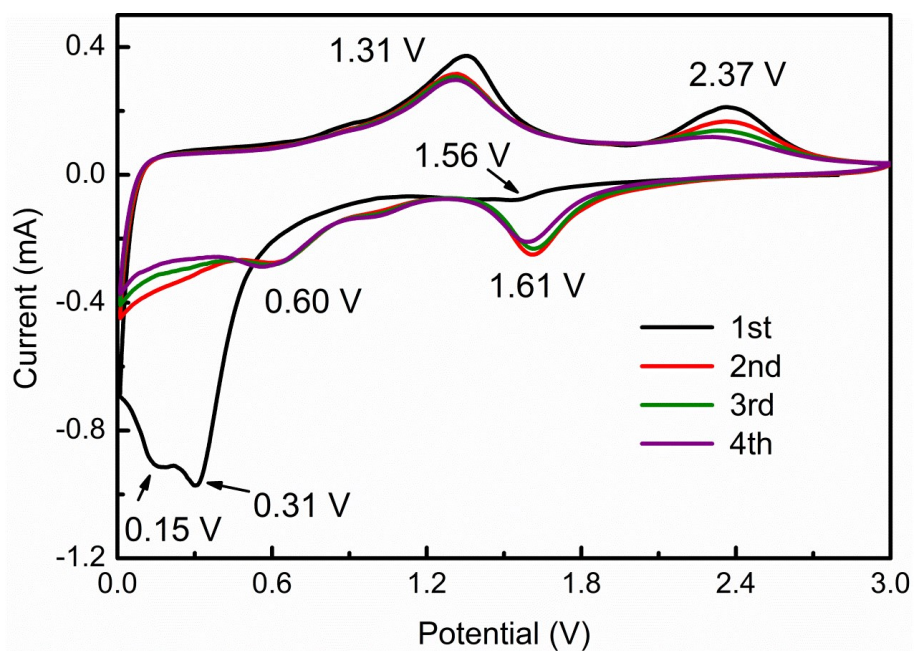


Figure S4. CV curves of the CVO-350 in the first four cycles.

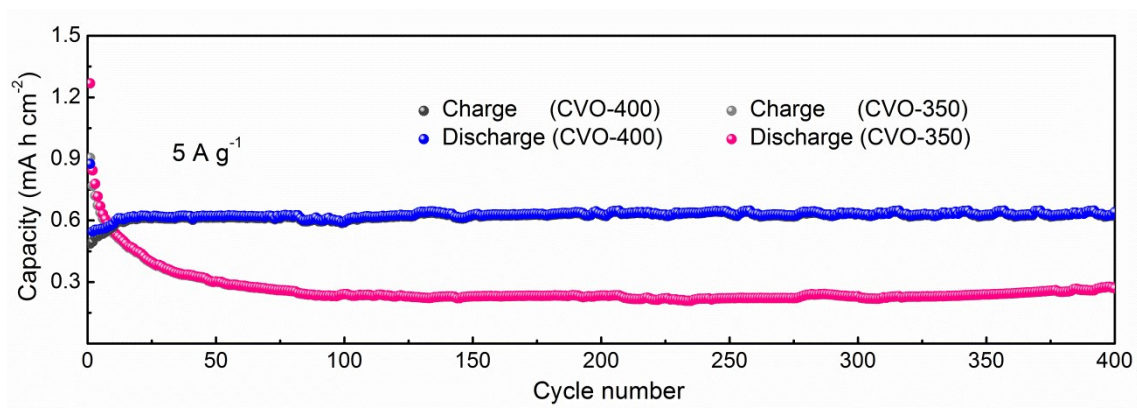


Figure S5. Areal capacities of the CVO-400 and CVO-350 electrodes at 5 A g^{-1} .

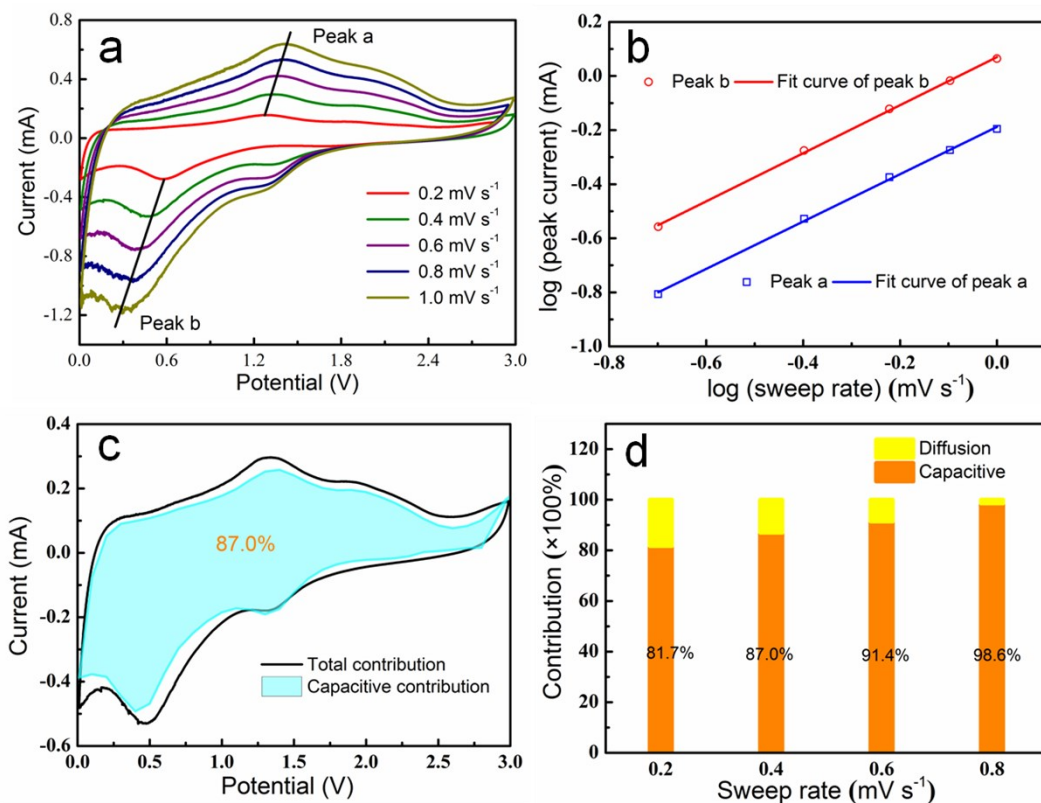


Figure S6. Kinetics analysis of CVO-400 for Li-ion storage: (a) CV curves at various scan rates from 0.2 to 1 mV s⁻¹, (b) calculated *b* values for cathodic and anodic peaks, (c) separation of the capacitive and diffusion currents at a scan rate of 0.4 mV s⁻¹ (the capacitive contribution to the total current is shown *via* the shaded region between the peak current and scan rate), (d) contribution ratios of the capacitive and diffusion-controlled charge at various scan rates.

The relationship between the measured current (*i*) and scan rate (*v*) can be expressed as the following equations^[S1]:

$$\log(i) = b \times \log(v) + \log(a)$$

where *a* and *b* are adjustable parameters. The power-law relationships between *i* and *v* are shown in Fig. S6b, in which the *b* values of CVO-400 are calculated to be 0.87 and 0.89 for the cathodic and anodic peaks, respectively, suggesting the predominant surface capacitive-controlled process of the kinetics. Furthermore, the ratio of the capacitive contribution can be calculated by the following equations^[S2]:

$$i(V) = k_1 v^{0.5} + k_2 v$$

$$i(V)/v^{0.5} = k_1 + k_2 v^{0.5}$$

where *k*₁ and *k*₂ can be easily determined by the relationship between *i*(*V*) and *v*^{0.5}. We quantify the capacitive contribution at a certain scan rate. From the result at a scan rate of 0.4 mV s⁻¹, 87% of capacity (shaded area) is contributed by the capacitive process.

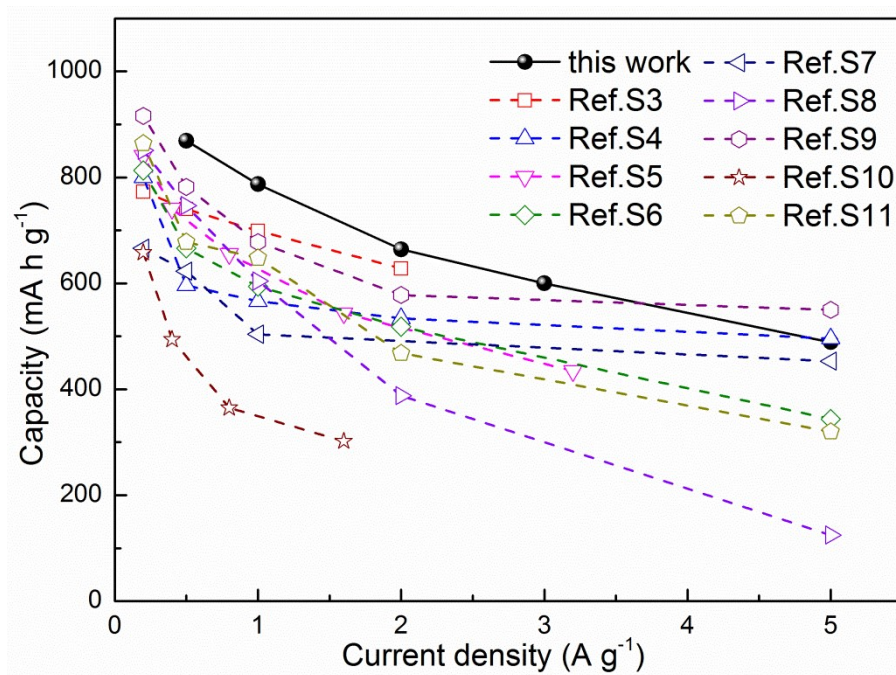


Figure S7. Capacities of CVO-400 and previously reported cobalt vanadates at varied current densities.

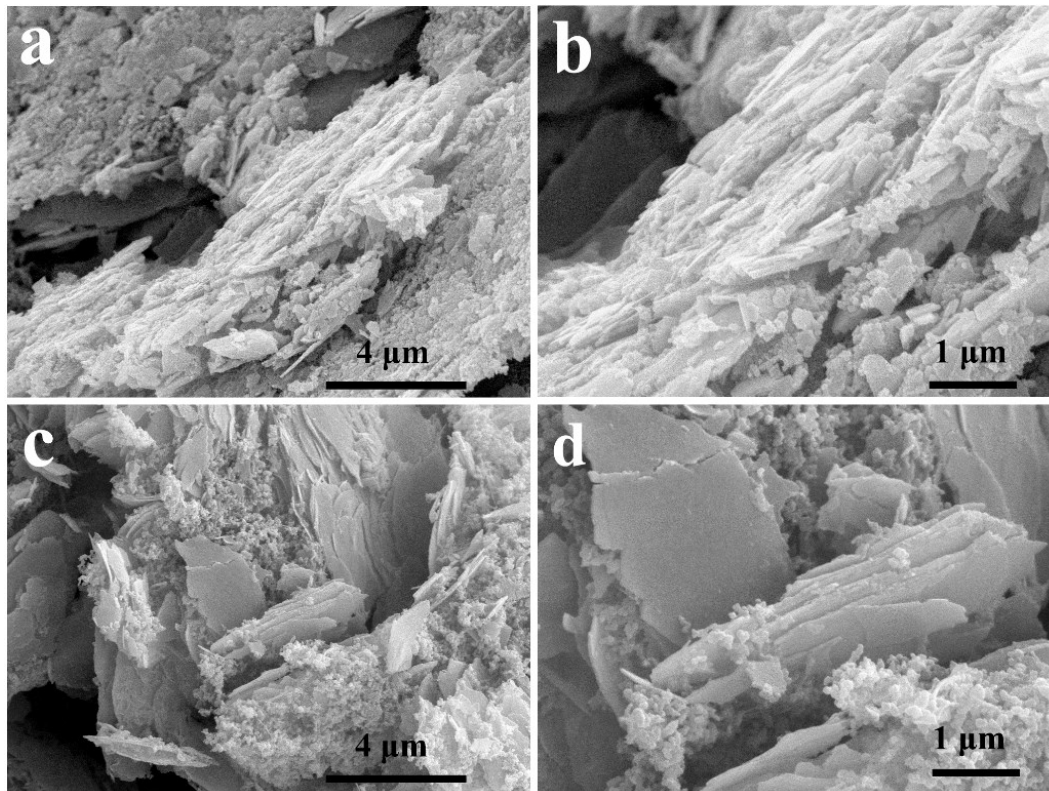


Figure S8. SEM images of CVO-350 and CVO-400 electrodes before cycling: (a, b) CVO-350, (c, d) CVO-400.

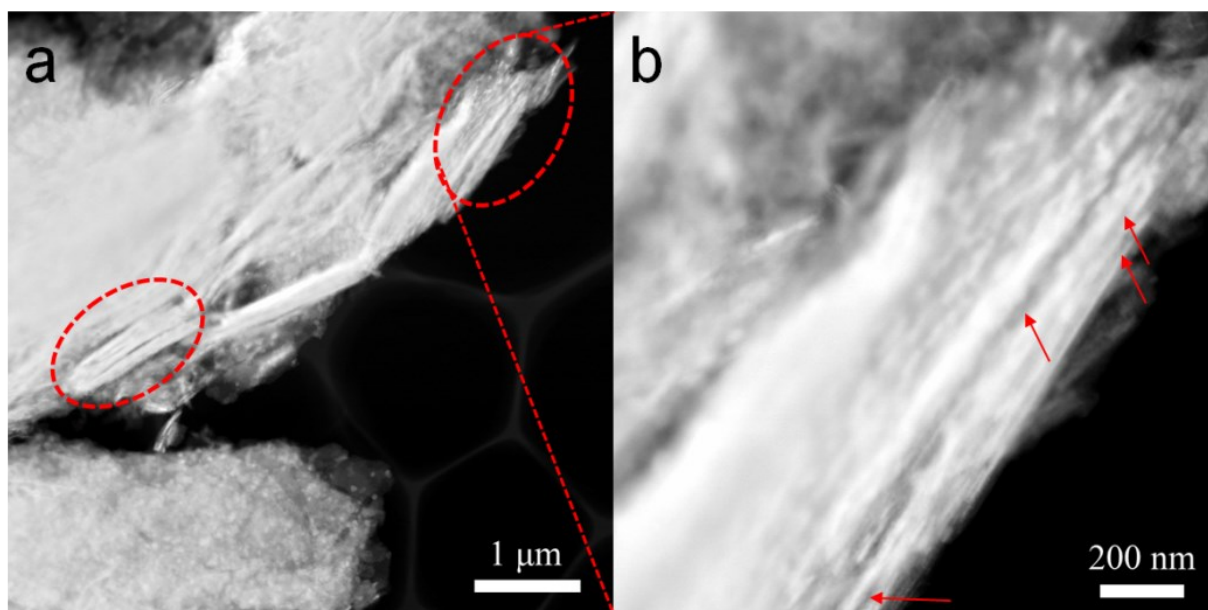


Figure S9. HAADF-STEM images of CVO-400 after cycling for 300 cycles.

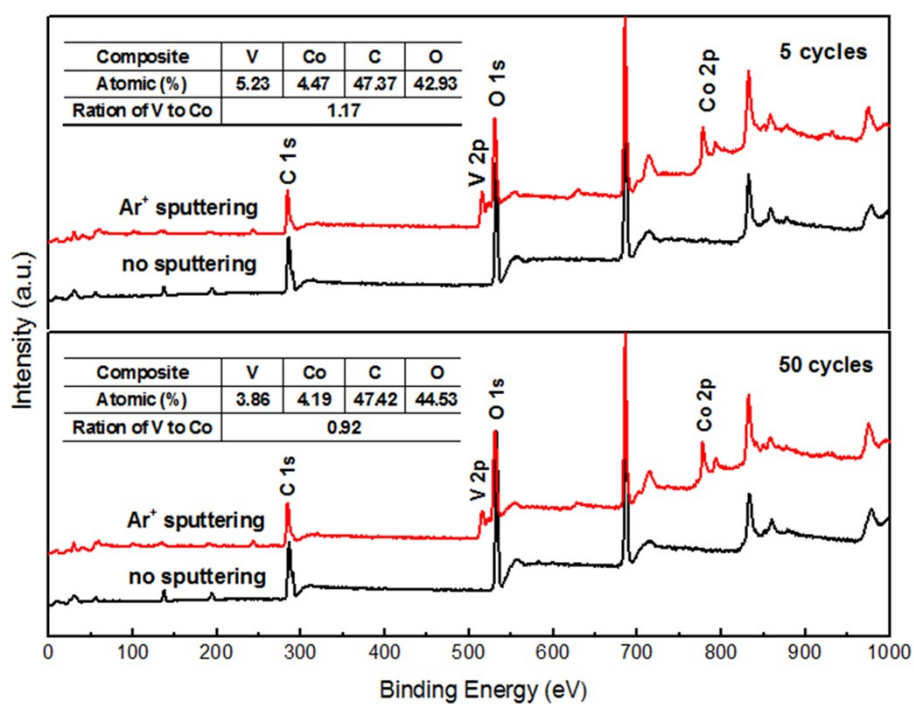


Figure S10. XPS depth analysis of active materials of CVO-400 in the 5th and 50th cycles, respectively.

To ensure the accuracy of the data, the disassembly of the batteries and the subsequent transfer of active materials were completed under the protection of Ar atmosphere. At the same time, in order to avoid the interference of surface components (electrolyte, SEI film), the surface of active substances were etched by Ar⁺ sputtering for 120 s before testing.

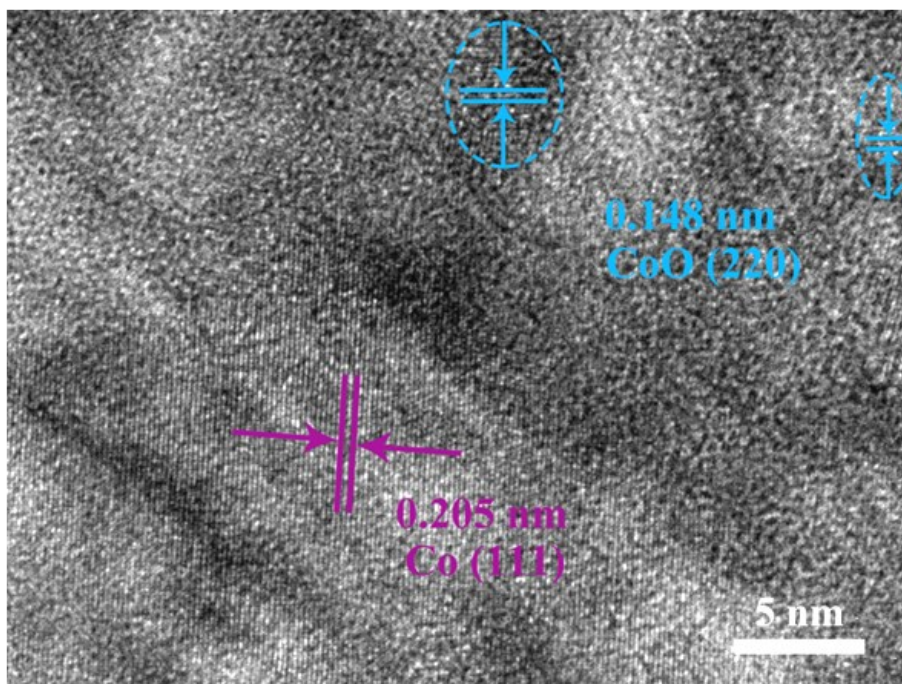


Figure S11. HRTEM image of CVO-400 at a current density of 1 A g⁻¹ after cycling for 100 cycles

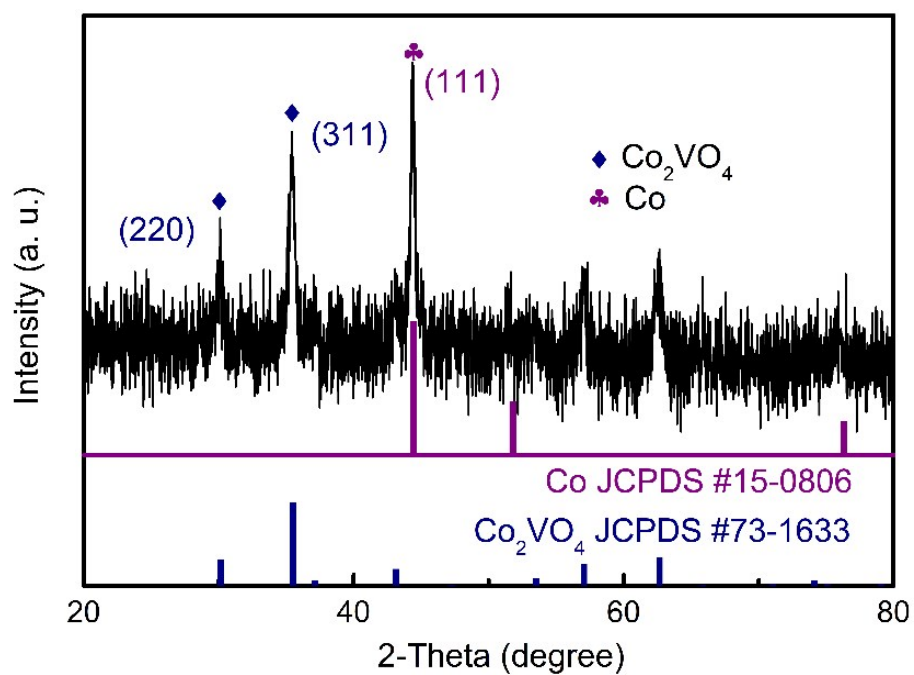


Figure S12. XRD pattern of the product calcined from the Co₂V₂O₇·3.3H₂O precursor at 600 °C (CVO-600)

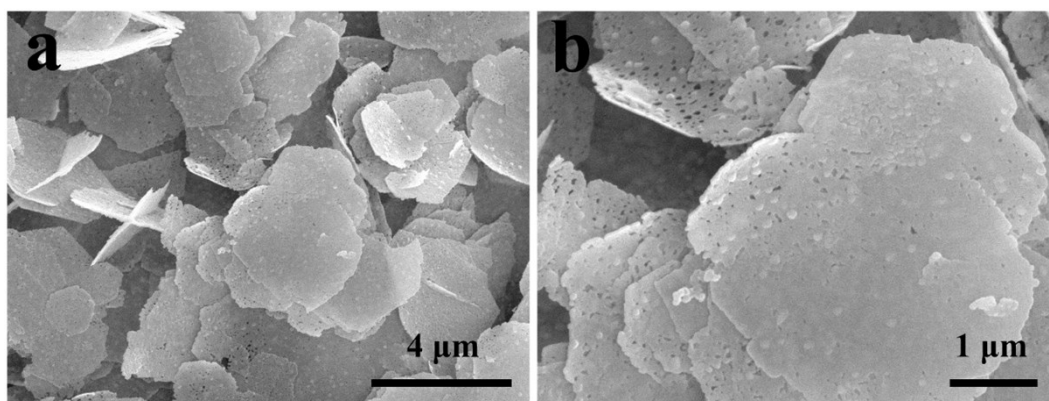


Figure S13. SEM images of CVO-600: (a) low magnification, (b) high magnification

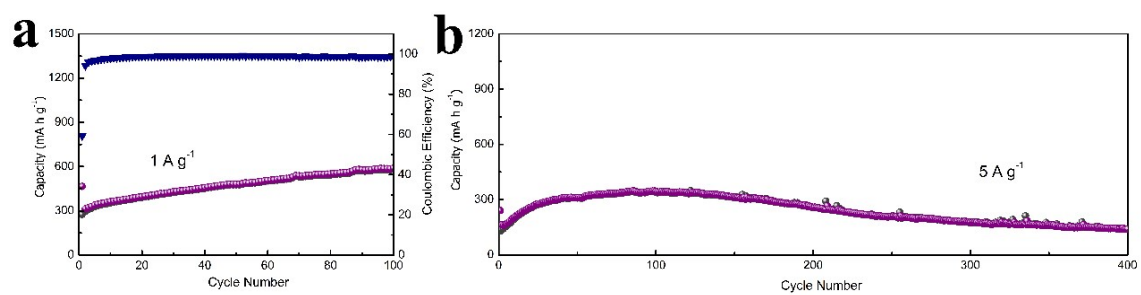


Figure S14. Cycling performances of CVO-600 at current densities: (a) 1 A g⁻¹, (b) 5 A g⁻¹.

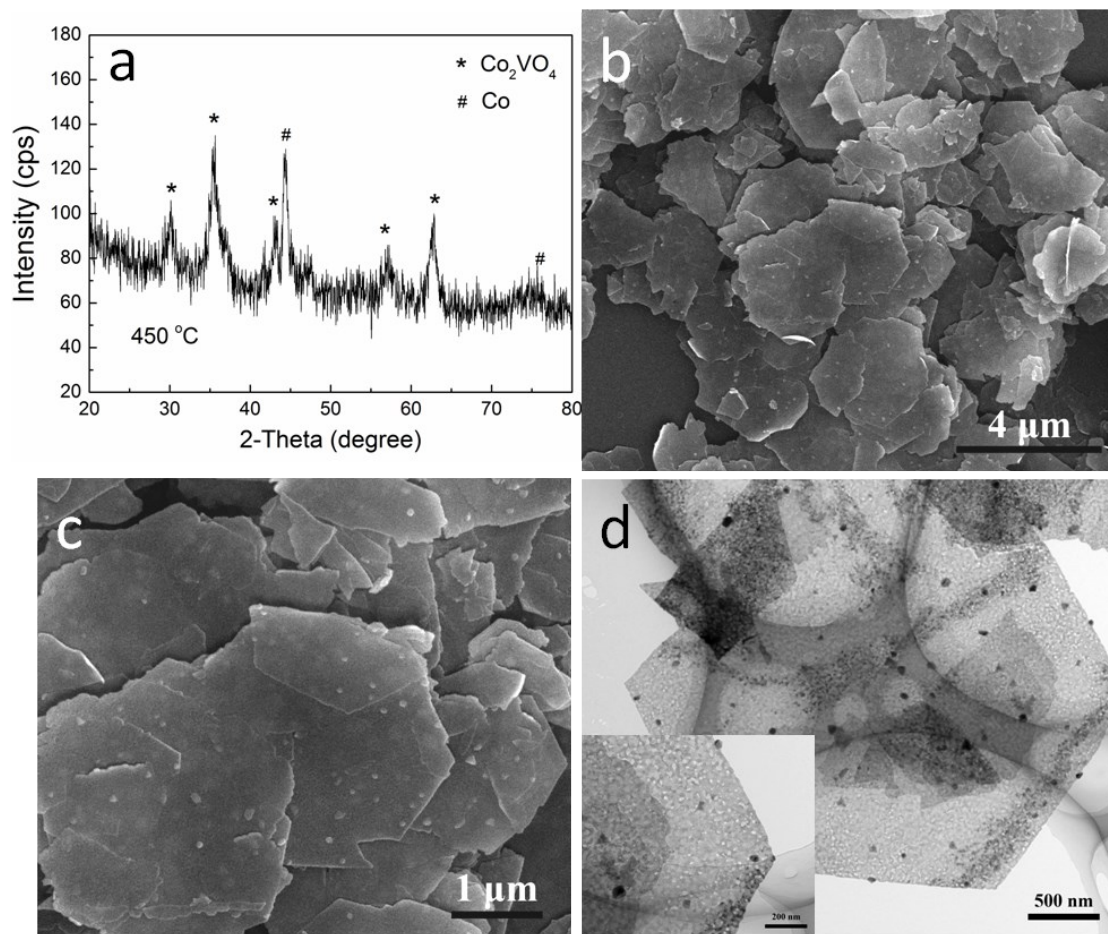


Figure S15. Microstructure characterizations of the product calcined from the $\text{Co}_2\text{V}_2\text{O}_7 \cdot 3.3\text{H}_2\text{O}$ precursor at $450\text{ }^\circ\text{C}$ (CVO-450): (a) XRD pattern, (b, c) SEM images, (d) TEM image.

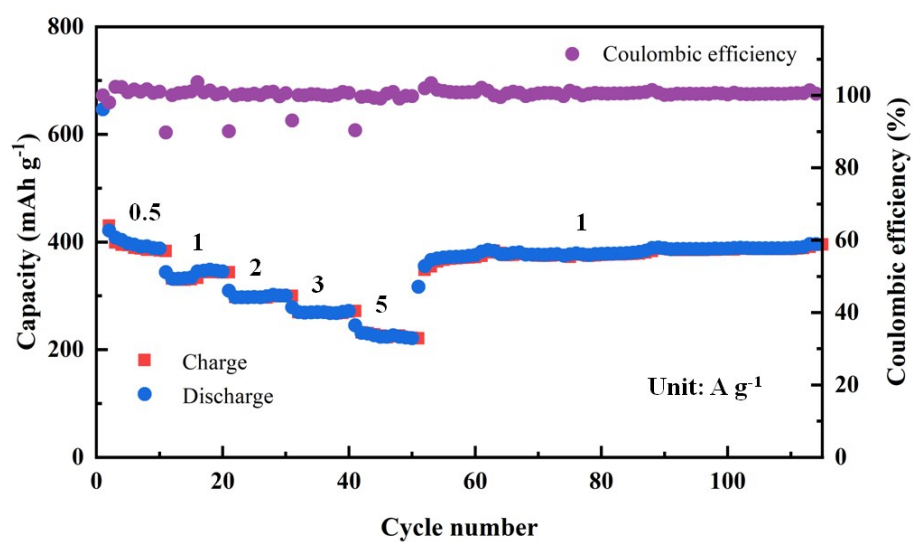


Figure S16. Rate performance of the CVO-450 electrode at varied current densities.

Table S1. Comparison of the Li-ion storage performance among the reported cobalt vanadate

anodes and our work.

| Materials and Structure | Reversible capacity | Cycling stability (remaining capacity/mA h g ⁻¹ , cycles, current density/A h g ⁻¹) | Ref. |
|--|---|--|--------------|
| Co/Co ₂ VO ₄ 2D-2D Heterostructure | 860 mA h g ⁻¹ at 0.5 A g ⁻¹ | 534, 400, 5 | This work |
| Co _{1.8} V _{1.2} O ₄ /rGO nanoparticles | 782 mA h g ⁻¹ at 0.2 A g ⁻¹ | 683, 300, 2 | S3 |
| Co ₃ V ₂ O ₈ ·nH ₂ O hollow hexagonal prismatic pencils | 960 mA h g ⁻¹ at 0.2 A g ⁻¹ | 847, 255, 0.5 | S4 |
| Co ₃ V ₂ O ₈ sponge network | 934 mA h g ⁻¹ at 0.2 A g ⁻¹ | 501, 700, 1 | S5 |
| Co ₂ V ₂ O ₇ mesoporous hexagonal nanoplatelets | 959 mA h g ⁻¹ at 0.5 A g ⁻¹ | 520, 580, 2 | S6 |
| CoV ₂ O ₆ macroporous nanosheets | 848 mA h g ⁻¹ at 0.2 A g ⁻¹ | 623, 500, 0.5 | S7 |
| CoV ₂ O ₄ | about 580 mA h g ⁻¹ at 0.2 A g ⁻¹ | 771, 100, 0.2 | S8 |
| Co ₃ O ₄ @Co ₃ V ₂ O ₈ hollow nanoboxes | 1186 mA h g ⁻¹ at 0.1 A g ⁻¹ | 706, 500, 1 | S9 |
| Co ₂ V ₂ O ₇ hollow cylinders | 1160 mA h g ⁻¹ at 0.1 A g ⁻¹ | 500, 180, 0.4 | S10 |
| Co ₃ V ₂ O ₈ nanotubes | 1479 mA h g ⁻¹ at 0.1 A g ⁻¹ | 630, 1100, 5 | S11 |

References:

- [S1] C. Chen, Y. Wen, X. Hu, X. Ji, M. Yan, L. Mai, P. Hu, B. Shan, Y. Huang, *Nat. Commun.* 2015, **6**, 6929.
- [S2] C. Yang, Y. Zhang, I. Zhou, C. Lin, F. Lv, K. Wang, J. Feng, Z. Xu, J. Li, S. Guo, *J. Mater. Chem. A* 2018, **6**, 8039.
- [S3] D. Zhang, G. S. Li, B. Y. Li, J. M. Fan, D. D. Chen, X. Q. Liu, L. P. Li, *Chem. Commun.* 2018, **54**, 7689.
- [S4] F. F. Wu, S. L. Xiong, Y. T. Qian, S. H. Yu, *Angew. Chem. Int. Ed.* 2015, **54**, 1.
- [S5] V. Soundharrajan, B. Sambandam, J. Song, S. Kim, J. Jo, S. Kim, S. Lee, V. Mathew, J. Kim, *ACS Appl. Mater. Interfaces* 2016, **8**, 8546.
- [S6] F. F. Wu, C. H. Yu, W. X. Liu, T. Wang, J. K. Feng, S. L. Xiong, *J. Mater. Chem. A*, 2015, **3**, 16728.
- [S7] L. Zhang, K. N. Zhao, Y. Z. Luo, Y. F. Dong, W. W. Xu, M. Y. Yan, W. H. Ren, L. Zhou, L. B. Qu, L. Q. Mai, *ACS Appl. Mater. Interfaces* 2016, **8**, 7139.
- [S8] J. S. Lu, I. V. B. Maggay, W. R. Liu, *Chem. Commun.* 2018, **54**, 3094.
- [S9] Y. Lu, L. Yu, M. H. Wu, Y. Wang, X. W. Lou (David), *Adv. Mater.* 2018, **30**, 1702875.
- [S10] J. L. Wang, J. Pei, K. Hua, D. H. Chen, Y. Jiao, Y. Y. Hu, G. Chen, *ChemElectroChem* 2018, **5**, 737.
- [S11] Z. Z. Qin, Ji. Pei, G. Chen, D. H. Chen, Y. Y. Hu, C. D. Lv, C. F. Bie, *New J. Chem.* 2017, **41**, 5974.